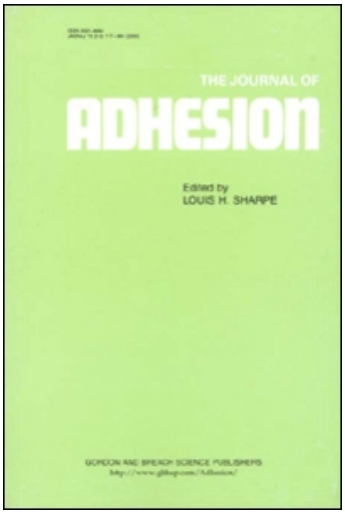

The Journal of Adhesion

Publication details, including instructions for authors and subscription information:
http://www.informaworld.com/smpp/title~content=t713453635

Mode-l Fracture Behaviour of Adhesive Joints. Part I. Relationship Between Fracture Energy and Bond Thickness

Hamid Reza Daghyani[a]; Lin Ye[a]; Yiu-Wing Mai[a]
[a] Centre for Advanced Materials Technology, Department of Mechanical and Mechatronic Engineering, The University of Sydney, Sydney, Australia

To cite this Article Daghyani, Hamid Reza , Ye, Lin and Mai, Yiu-Wing(1995) 'Mode-l Fracture Behaviour of Adhesive Joints. Part I. Relationship Between Fracture Energy and Bond Thickness', The Journal of Adhesion, 53: 3, 149 — 162
To link to this Article: DOI: 10.1080/00218469508009935
URL: http://dx.doi.org/10.1080/00218469508009935

J. Adhesion, 1995, Vol. 53, pp. 149–162
Reprints available directly from the publisher
Photocopying permitted by license only

Mode-I Fracture Behaviour of Adhesive Joints. Part I. Relationship Between Fracture Energy and Bond Thickness

HAMID REZA DAGHYANI, LIN YE*and YIU-WING MAI

Centre for Advanced Materials Technology, Department of Mechanical and Mechatronic Engineering, The University of Sydney, Sydney, NSW 2006, Australia

(Received July 4, 1994; in final form February 16, 1995)

The fracture properties of adhesive joints of aluminium were investigated using a rubber-modified tough epoxy resin system ($G_{IC} = 2.76\,kJ/m^2$) as adhesive material. Compact tension (CT) adhesive joints were manufactured for a wide range of bond thickness t (from 0.05 mm to 10 mm) and fracture tests conducted under static load. Scanning electron microscopy (SEM) was used to examine the fracture surface morphology. A large deformation elastic- plastic finite element model was developed to evaluate the J-integral value for different bond thickness. The fracture energy, J_C, was found to be highly dependent on the bond thickness and was lower than that of the bulk adhesive. As the bond thickness was increased J_C also increased, though not monotonically, towards the fracture energy of the bulk adhesive. This result was caused by the complicated interactions between the stress and strain fields, plastic deformation of the adhesive around the crack tip, constraint from the adherends and the failure path. It was shown that values of J_C as a function of bond thickness correlated well with the variation of plastic zone height. Scanning electron micrographs from the fracture surfaces of the CT adhesive joints illustrated that the failure path was mainly cohesive through the centre-plane of the adhesive layer. Brittle fracture mechanisms were observed for thin bonds ($0.04\,mm < t < 0.5\,mm$) but tough fracture mechanisms were identified for thick bonds ($t > 1\,mm$).

KEY WORDS adhesive joints; bond thickness; mode-I fracture toughness; finite element analysis; epoxy resin; fractography.

1 INTRODUCTION

Adhesive joints have been widely used over the last few decades in aerospace and civil engineering structures with both technical and economic benefits. Among the many materials used for modern structural adhesives, rubber-modified epoxies are most prominent. Many studies have been carried out to identify the effects of bond thickness on the fracture energy of adhesive joints[1–12] covering both thin (less than 1 mm)[1–7] and thick[8,9] adhesive layers. Unfortunately, no simple relationship between fracture energy and bond thickness exists. Hunston and Bascom[4] found that, for a particular rubber-modified epoxy adhesive, the fracture energy, G_{IC}, was maximum at a bond thickness between 0.5 to 0.7 mm. These results were mainly attributed to the variation of the

* Corresponding author.

plastic zone size formed at the crack tip. It was also proposed that the translation of the matrix toughness to fibre-reinforced composites was limited by the formation of the crack tip plastic zone and its size, which in turn was determined by the constraint created by the fibre spacing in the composite. Conversely, Chai[5,6] observed that the fracture energy in the range of very thin bonds, less than 0.05 mm, decreased with increasing bond thickness for a somewhat different reason. That is, the main fracture energy dissipation mechanism was not directly related to the crack tip plastic zone size but to the different fracture surface morphology. These studies highlight the need to perform a comprehensive investigation on the effect of the both crack tip plastic deformation and fracture morphology in adhesive joints of different bond thickness.

In the present work, a large deformation elastic-plastic finite element model was developed and the morphology of fracture surfaces was examined to assess the fracture behaviour of a rubber-modified epoxy which was used as an adhesive material in aluminium joints for a range of bond thickness. A comprehensive crack tip stress analysis was further conducted to evaluate the relationship between plastic constraint and fracture behaviour of adhesive joints. This is given in Part II of this paper.[21]

2 EXPERIMENTAL PROCEDURE

2.1 Materials and Specimen Preparation

The base adhesive material was a diglycidyl ether of bisphenol A (DGEBA) epoxy resin (Araldite® GY260, supplied by Ciba-Geigy, Australia) modified with a liquid rubber (CTBN, 1300 × 13, BFGoodrich). The curing agent was piperidine, in a ratio of 5:100 (by wt.) mixed with the pure resin. The properties of this adhesive material have been reported previously.[13] It was found that the fracture energy of the pure GY260 epoxy resin was maximised with only 2% rubber. Table I shows some fracture and mechanical properties of the cured pure GY260 resin system and for the system modified with 2% rubber. The rubber-modified epoxy was prepared by first adding the CTBN rubber to the DGEBA epoxy resin by hand-mixing for about 5–10 minutes, and degassing the mixture in a vacuum oven (−80 kPa) at 60°C. Piperidine was then added to the mixture with minimum air entrapment. Adhesive joints based on compact tension (CT)

TABLE I

Mechanical properties of pure GY260 epoxy resin and its 2% rubber-blended system

Resin System	Hardener	σ_T	E	ε_t	G_{IC}	ρ	T_g
		MPa	GPa	%	J/m^2	g/Cm^3	°C
GY260	Piperidine	82	3.3	3.6	1760	1.15	80.1
GY260 + 2% Rubber	Piperidine	81.5	3.1	4.8	2760	–	83.9

σ_T: Tensile yielding strength
E : Young's modulus
ε_t : Elongation to break
G_{IC} : Fracture toughness
ρ : Density
T_g: Glass transition temperature

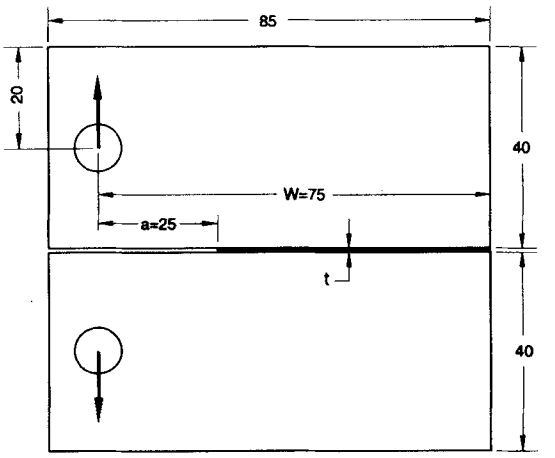

FIGURE 1 Schematic illustration of CT adhesive joint (t is bond thickness). All dimensions in mm.

specimens, Figure 1, were prepared from adherends made of 6061 aluminium alloy 8 mm thick. The surfaces of the adherends to be bonded together were first ground using a 400 grit paper, degreased with acetone, and then cleaned in an alkaline solution. Subsequently, these surfaces were subjected to the P2 etching procedure with a sulfo-ferric solution and finally dried in clean air.[14] The bond thickness (from 0.05 mm to 10 mm) of the CT adhesive joints was controlled by two spacers located at both ends of the bond line. Pre-cracks ($a/W = 1/3$) were introduced at the centre of the bond thickness with a 20 μm Teflon film. All sides of the bond line were sealed by a sticky tape except a small opening. The specimen was then preheated in an oven for 15 minutes at 120°C and the resin was cast through this opening. The CT adhesive joints were finally cured for 16 h at 120°C. After curing, the edges of the bond line were polished.

2.2 Testing Procedure

All CT specimens were tested in an Instron model 4302 machine at ambient temperature with a crosshead speed of 0.3 mm/min. The fracture surfaces were first stained with osmium tetroxide (OSO_4) to enhance contrast and then coated with a thin layer of platinum to increase surface conductivity. A JEOL 35C scanning electron microscope (SEM) with an accelerating voltage of 15 kV was employed for fractographic studies.

3 FINITE ELEMENT MODELLING

A large deformation and elastic-plastic finite element model (FEM) was developed to estimate J-integral values of the CT adhesive joints with different bond thickness. All finite element analyses (FEA) were carried out by assuming linear-elastic behaviour for the aluminium adherends and elastic-plastic behaviour for the adhesive. Figure 2 shows the stress-strain curve of the bulk adhesive material determined from experi-

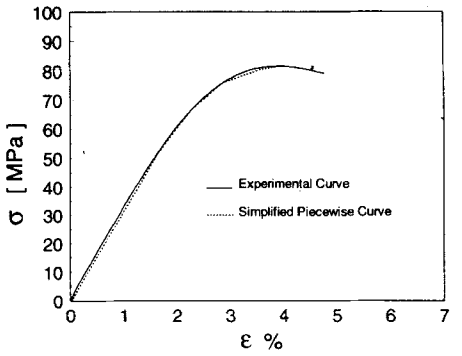

FIGURE 2 Uniaxial tensile stress strain curve of adhesive material.

ments,[13] which was simplified to a piecewise curve for the finite element analysis. The J-integral was evaluated from the stress and strain fields around the crack tip based on the Rice[15] J-contour integration method, *i.e.* the J-integral was defined by an integration along an arbitrary counter-clockwise path (Γ) around a crack tip given by:

$$J = \int_{\Gamma} [W(\varepsilon)\mathbf{dy} - T_i \frac{\partial u_i}{\partial x} ds] \tag{1}$$

where $W(\varepsilon)$ is the strain energy density, T_i the traction vector, u_i the displacement vector and ds a length increment along the contour Γ. ABAQUS software[16] was used for the evaluation of the path-independent J-integral. Figure 3 shows a typical FEM mesh of the CT specimen. Because of symmetry only one-half of the geometry was considered. For the adherend coarse meshes were used, but fine meshes and singular elements were employed around the crack tip. All meshes were generated by plane-strain[7,17,18] eight-noded quadrilateral elements with nine-point integration in element evaluation.

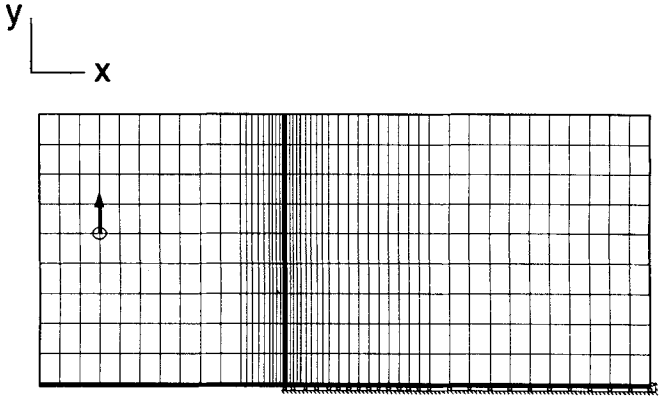

FIGURE 3 Finite element model for a typical CT adhesive joint.

4 RESULTS AND DISCUSSION

4.1 Effect of Bond Thickness on Fracture Toughness

A range of bond thickness was examined to assess the constraint effect on the fracture energy of the adhesive material. The critical loads (which coincided with the maximum loads) obtained from experiments at fracture of the CT adhesive joints were used to evaluate the crack growth resistance. Figure 4 shows the critical load, P_C, *versus* bond thickness, t, which can be classified into three distinct regimes. When $0.04\,\text{mm} < t < 0.5\,\text{mm}$, a moderate increase in the critical load (P_C) was observed, while for $0.5\,\text{mm} < t < 1\,\text{mm}$, P_C was found to rise dramatically, peaking at $t = 1\,\text{mm}$. Further increase in the bond thickness ($t > 1\,\text{mm}$) resulted in a gradual drop of P_C. At $t = 10\,\text{mm}$, P_C was still higher than the critical load at fracture of the bulk adhesive material with the same specimen geometry and identical starting crack length. The relationship between the critical load of adhesive joints and that of the bulk adhesive material can be described by the restriction of the high stiffness adherends on the extent of plastic deformation of the adhesive material.

The critical loads determined by the experiments were used in the finite element model to estimate the critical J-integral, *i.e.* J_C. Figure 5 shows J_C as a function of t. The major fracture mechanism of the bulk adhesive material was identified in a previous paper.[13] Scanning electron microscopy (SEM) conducted on fracture surfaces of the bulk rubber-modified epoxy indicated a considerable plastic deformation at the crack tip due to shear yielding. Shear slip lines initiating from the crack tip were also observed using polarised light in a transmission microscope on a thin section sample which was taken from a region containing the arrested crack produced by four-point bending specimens with double notches. Furthermore, detailed SEM examinations from some areas with large plastic deformation revealed very small dispersed rubber particles ($< 0.1\,\mu\text{m}$) which, however, did not have any effect on the fracture toughness.[19,20] Therefore, shear yielding is the governing fracture mechanism in the bulk adhesive material.

The fracture surfaces of all the CT specimens with different bond thickness exhibited essentially cohesive failure in the adhesive layer. However, at crack initiation, in some

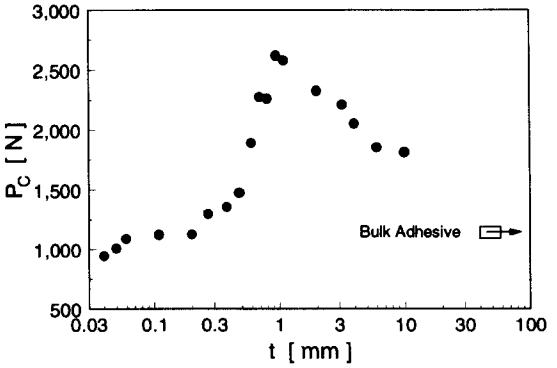

FIGURE 4 Variation of critical load *versus* bond thickness.

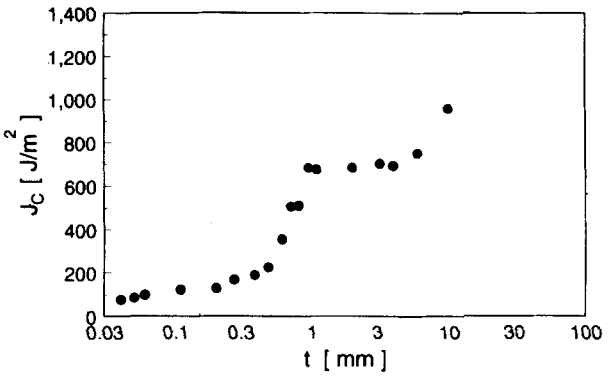

FIGURE 5 Relation between J_C and bond thickness obtained from FEA.

specimens, the fracture was preceded by shear yielding in a direction about 45° to the crack plane and then propagated very close to the adherend for a small distance. Thereafter, the failure path was mainly cohesive through the adhesive layer. This failure mechanism was attributed to the high tri-axial stress state around the crack tip, which controls shear yielding in the adhesive material. A comprehensive elastic-plastic stress analysis in these adhesive joints and the crack tip stress field are given in Part II of this paper.[21] It is proposed that because of the constraint imparted by the adherends, a high hydrostatic tension occurred inside the crack tip plastic zone. The effects of hydrostatic stresses on shear yielding of polymers have been proposed by some investigators[19,20] based on a modified Von-Mises yield criterion given by:

$$\tau_{oct} = \tau_y - \mu\sigma_m \tag{2}$$

where τ_{oct} is the octahedral shear stress, τ_y is the yield stress in pure shear, μ is a material constant and an indication of the sensitivity of the material to the hydrostatic stress component, and σ_m is the hydrostatic tension given by:

$$\sigma_m = \frac{1}{3}(\sigma_1 + \sigma_2 + \sigma_3) \tag{3}$$

where $\sigma_i (i = 1, 2, 3)$ are the principal stress components. Eq. (2) suggests that decreasing the hydrostatic tension leads to a high octahedral shear stress. Associated with shear yielding of the adhesive material, this stress state will produce a plastic zone around the crack tip. But this high shear stress state is quickly relieved along the crack path behind the crack tip.[21,22] Furthermore, the octahedral shear stresses may produce a severe shear deformation to cause local damage near the crack tip. Figures 6a and 6b show the fracture surfaces of the adhesive joint specimens. The crack may propagate initially very close to the adherend/adhesive interface, as shown in the pictures, but finally it produced a fast fracture near the mid-plane of the adhesive layer.

Based on the bond thickness, the fracture behaviour (as indicated in Fig. 5) can be divided into the following regimes: (i) 0.04 mm $< t <$ 0.5 mm, (ii) 0.5 mm $< t <$ 1 mm, (iii) 1 mm $< t <$ 4 mm, and (iv) $t >$ 4 mm. The relationship between J_C and t is similar to that between P_C and t when $t <$ 1 mm, but the correlation is somewhat different for

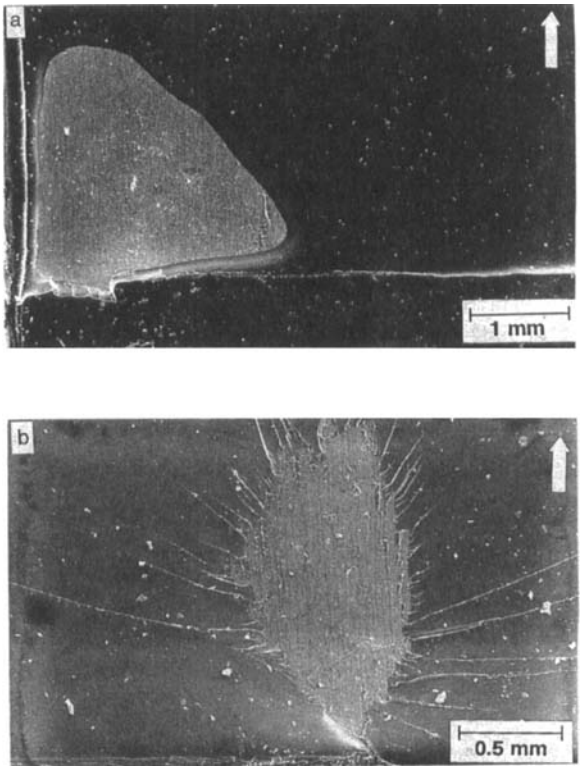

FIGURE 6 Fracture surfaces (a) $t = 0.2$ mm and (b) $t = 0.6$ mm. (Arrow indicates crack growth direction; light areas indicate fracture close to the adherend surface).

larger bond thickness. J_C approaches a plateau value when $1\,\text{mm} < t < 4\,\text{mm}$, but it increases sharply after $t > 4$ mm. This trend indicated that by increasing the bond thickness, the constraint effect from the adherends is reduced, which results in larger deformation zones and, therefore, more energy absorption.

SEM studies on the fracture surfaces have revealed some special fracture characteristics for the adhesive joints with different bond thickness:

(i) 0.04 mm < t < 0.5 mm

The fracture surfaces in this range of bond thickness are mostly quite smooth, typical of brittle failure. When $0.04\,\text{mm} < t < 0.06\,\text{mm}$, the crack was mainly cohesive through the mid-thickness of the adhesive layer, though in some areas it proceeded along the plane adjacent to the adhesive/adherend interface. Figures 7a and 7b show the fracture surfaces for $t = 0.05$ mm in regions with a thick layer of adhesive and near the adhesive/adherend interface. A magnified view of the adhesive/adherend interface region, Figure 7c, indicates that the adherend was covered with mainly thin pieces of the adhesive resin, confirming that the failure of the adhesive joint is cohesive. For $0.06\,\text{mm} < t < 0.5\,\text{mm}$, a small part of the pre-crack may initiate in a direction about

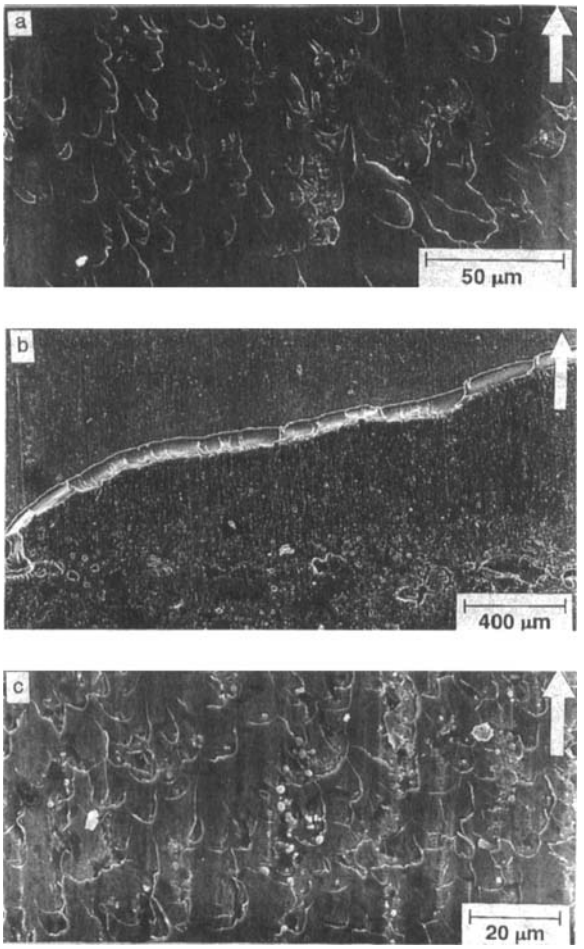

FIGURE 7 Fracture surfaces of adhesive joints with thin bond thickness ($t = 0.05$ mm). (a) Surface with a thick layer of adhesive, (b) surface showing transition from cohesive to adhesive/adherend interface, and (c) magnified view of the adhesive/adherend interface. (Arrow indicates crack growth direction).

45° to the fracture plane until the crack reaches the adhesive/adherend interface. Then the crack jumps back and proceeds along the mid-plane of adhesive layer. (See Fig. 6a). Figure 8a shows the fracture surface with a transition line between failure at the adhesive/adherend interface and the adhesive for $t = 0.2$ mm. However, the fracture surface at the adhesive/adherend interface is, in fact, coated with thin pieces of the adhesive resin (Fig. 8b) similar to $t = 0.05$ mm. (See Fig. 7c).

(ii) 0.5 mm < t < 1 mm

As the bond thickness is increased the constraint effect from the adherends is decreased. Therefore, more plastic energy absorption takes place at the crack tip. Stress analysis in adhesive joints[21–24] revealed that, for the same external applied load in the CT and

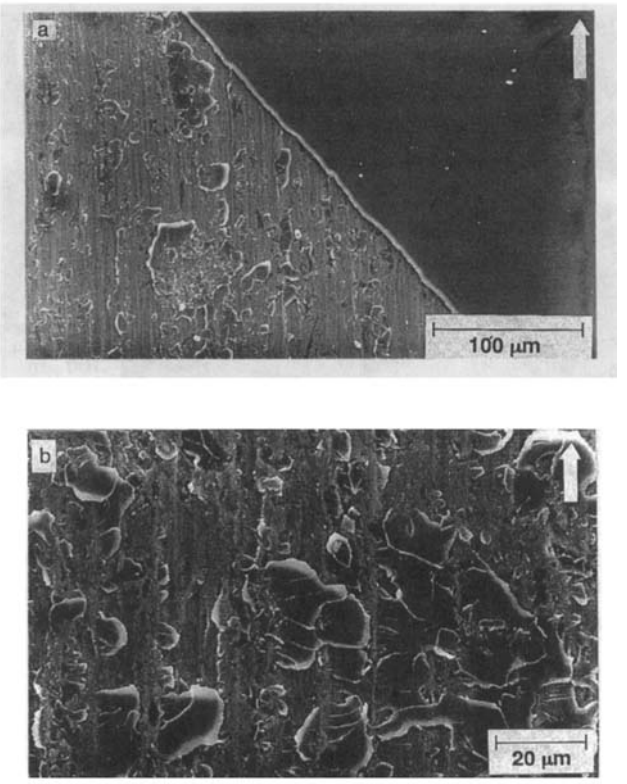

FIGURE 8 Fracture surfaces of adhesive joints with medium thickness ($t = 0.2$ mm). (a) Surface with cohesive failure and along the adhesive/adherend interface, and (b) adhesive/adherend interface coated with thin pieces of epoxy resin. (Arrow indicates crack growth direction).

DCB specimens containing the same crack length, the stresses at the crack tip are lower for larger bond thickness. This means that for joints with a large bond thickness the adhesive material undergoes more plastic deformation which relieves the high hydrostatic stress. According to Eq. (2) it is easier to satisfy the yielding criterion so that there is extensive shear yielding and consequently more energy dissipation with higher J_C. Figure 9 shows the plastic deformation lines in a region near the crack tip for $t = 0.6$ mm. The fracture surface for $t = 1$ mm is shown in Figure 10a. Half of the fracture surface is near the adhesive/adherend interface and the other half is cohesive failure in the adhesive material when $t = 1$ mm. Comparison of Figures 10a and 8a shows that there is more plastic deformation in the adhesive joint with a larger bond thickness.

(iii) $1 < t < 4$ *mm*

Even though the critical load is decreased in this range of bond thickness, J_C is approximately constant. (See Fig. 5). Whilst the critical load is reduced for joints with large bond thickness, leading to lower crack tip stresses, the larger plastic deformation

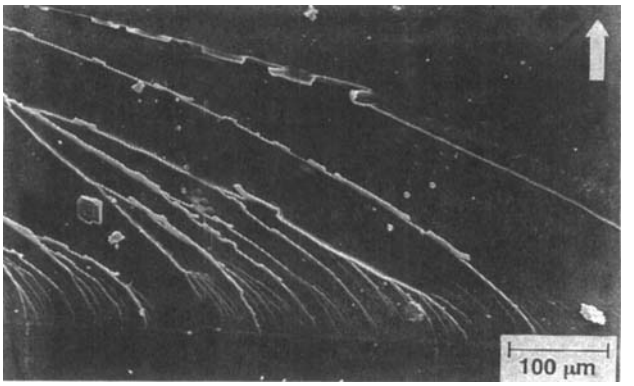

FIGURE 9 Plastic deformation lines ahead of the crack tip for $t = 0.6$ mm. (Arrow indicates crack growth direction).

has, however, continued to produce a constant J_C. Figure 10b represents the fracture surface for $t = 2$ mm. Notice that the failure mechanisms are similar to those for $t = 1$ mm as shown in Figure 10a.

(iv) $t > 4$ mm

For $t > 4$ mm J_C increases sharply towards the fracture energy of the bulk adhesive material ($J_C = 2.76$ kJ/m^2). Also, from Figure 4 it is clear that P_C approaches the critical load for the bulk adhesive material. These results are caused by further reduction of the plastic constraint from the adherends, which promotes an extensive plastic deformation field around the crack tip leading to large scale yielding in the adhesive material. Figure 11a shows the amount of plastic deformation[25] in the stable crack growth region formed in front of the pre-crack and followed by fast fracture for $t = 10$ mm. Compared with the same region in the bulk adhesive material as shown in Figure 11b,[13] it is seen that the stable crack growth region is much smaller. Therefore, the constraint provided by the adherends still restricts the material deformation even for the joint with a very large bond thickness. Consequently, the fracture energy is still lower than that of the bulk adhesive material.

4.2 Comparisons Between Present and Previous Results

It was shown in previous work that the correlations between the fracture energy and the adhesive bond thickness are very complicated. Although Hunston and Bascom[4] and Chai[5] have found a maximum mode-I fracture energy at some particular bond thickness, other investigators[7-12] reported that no maximum fracture energy can be obtained. Furthermore, it is stated in some studies[4] that the fracture energy is directly related to the size of the crack tip plastic zone, and its variation with bond thickness is determined by the constraint effect from the adherends. However, it is also noted that[5,6] for some bond thickness, especially in the range of very thin bonds

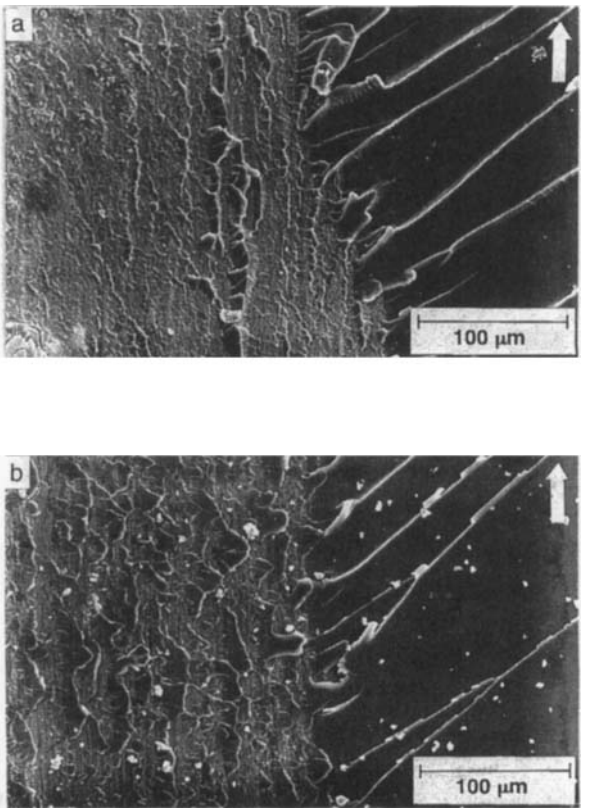

FIGURE 10 Fracture surfaces for (a) $t = 1$ mm and (b) $t = 2$ mm. The right hand side of these photos show cohesive fracture in the adhesive material and the left hand side shows the adhesive/adherend interface. (Arrow indicates crack growth direction).

($t < 0.05$ mm), the fracture energy is reduced, despite the increase in bond thickness with a corresponding reduction in the constraint effect. The reason for the trend of these different results is attributed to the difference in the fracture surface morphology.

In the present study, the fracture energy, J_C, evaluated by the FEA model generally is increased as t is increased. A rapid rise in J_C occurs in the range $0.5\,\text{mm} < t < 1\,\text{mm}$; then J_C reaches a steady state value. Further increase in t enables J_C to approach the value for the bulk adhesive material. In the regime of small bond thickness. ($0.04\,\text{mm} < t < 0.5\,\text{mm}$), the high constraint from the adherends causes the adhesive material to fail in brittle fashion. Therefore, the relief of the plastic constraint at the crack tip results in a gradual increase of J_C when the bond thickness is increased. However, for $0.5\,\text{mm} < t < 1\,\text{mm}$, the adhesive material goes through a considerable plastic deformation at the crack tip as evidenced by the pronounced plastic flow on the fracture surfaces. This leads to a sharp rise in J_C in this bond thickness range because of the high fracture energy of the bulk adhesive material.

An important result obtained here is that J_C for different bond thickness ($0.04\,\text{mm} < t < 10\,\text{mm}$) are always less than the fracture energy of the bulk adhesive

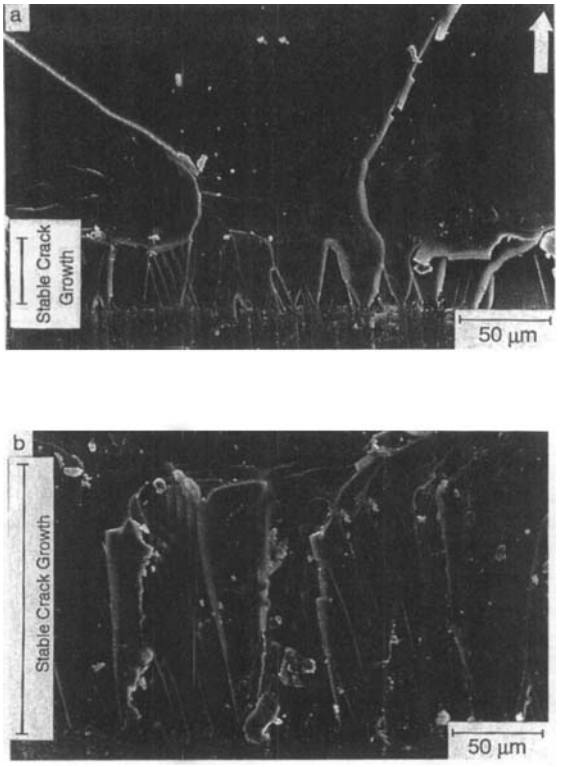

FIGURE 11 Plastic deformation in the stable crack growth zones formed ahead of the crack tip for (a) $t = 10$ mm, and (b) bulk adhesive material. (Arrow indicates crack growth direction).

material. Although the fracture energy of some adhesive joints has been found to be very close to that of the bulk adhesive material at some particular bond thickness,[4,5] there has been insufficient explanation as to why the fracture energy is lower than the bulk adhesive at other different bond thickness.[12,26] The adhesive materials referred to are mostly rubber-modified epoxy systems in which toughening mechanisms such as rubber cavitation, rubber stretching and shear band formation may contribute to the fracture energy.[27,28] In the absence of these mechanisms, such as in the adhesive material studied here, the fracture process is largely controlled by the plastic deformation around the crack tip caused by shear yielding of the epoxy resin. The aluminium adherends restrict the formation of the plastic zone and lower the fracture energy. Since the constraint from the adherends in the joints is higher than that in the bulk adhesive material,[21] the fracture energy in such adhesive joints is lower.

The fracture energy of adhesive joints is generally influenced by the fracture path, *e.g.* cohesive within the adhesive layer and/or an interfacial failure between adhesive and adherend. A cohesive failure gives a higher fracture energy than an interfacial failure.[5,6] Consequently, the fracture toughness of the adhesive joints with different bond thickness may be affected by the following factors: (a) failure path which depends on the surface preparation of the adherends and, consequently, on the bonding strength

between adhesive and adherends; (b) constraint from adherends which controls the stress state and the deformation field of the adhesive material around the crack tip; and (c) energy dissipation mechanisms around the crack tip in the adhesive material, which are related to the morphology of the fracture surfaces.

5 CONCLUSIONS

The fracture behaviour of compact tension joints of adhesively-bonded aluminium of different bond (adhesive) thickness with a rubber-toughened resin as adhesive material was investigated using SEM on the fracture surfaces and elastic-plastic finite element analyses (FEA). The critical J-integral, J_C, evaluated by FEA, indicated a complicated trend with the bond thickness, t. For $0.04\,\text{mm} < t < 0.5\,\text{mm}$, J_C increased gradually (from $75\,\text{J/m}^2$ to $225\,\text{J/m}^2$) with t; however, for $0.5\,\text{mm} < t < 1\,\text{mm}$, J_C rose sharply (from $225\,\text{J/m}^2$ to $685\,\text{J/m}^2$). In the range $1\,\text{mm} < t < 4\,\text{mm}$, J_C was almost constant; whilst for $t > 4\,\text{mm}$, J_C increased gradually towards the fracture energy of the bulk adhesive material ($J_C = 2.76\,\text{kJ/m}^2$). SEM micrographs show some different local failure mechanisms at crack initiation. However, crack propagation was generally through the mid-plane of the adhesive layer and, hence, the fracture path was fully cohesive. For small bond thickness with high constraint ($0.04\,\text{mm} < t < 0.5\,\text{mm}$), the fracture surfaces were characteristically brittle. But for large t the fracture surfaces showed features consistent with high toughness. Therefore, for the rubber-modified epoxy used in this study, the relationship between the fracture energy and bond thickness is mainly controlled by the amount of crack tip plastic deformation as may be influenced by the constraint imposed by the adherends.

Acknowledgements

Thanks are due to Dr. S. X. Wu for his assistance in finite element analysis and to the Electron Microscope Unit at the University of Sydney for access to its facilities.

References

1. S. Mostovoy and E. J. Ripling, *J. Appl. Polym. Sci.* **15,** 661 (1971).
2. S. Mostovoy, E. J. Ripling and C. F. Bersch, *J. Adhesion,* **3,** 125 (1971).
3. A. J. Kinloch and S. J. Shaw, *J. Adhesion,* **12,** 59 (1981).
4. D. L. Hunston and W. D. Bascom, *ACS Advances in Chemistry Series No. 208: Rubber-Modified Thermoset Resins,* C. K. Riew and J. K. Gillham, Eds. (Amer. Chem. Soc., Washington, 1984), pp. 83–99.
5. H. Chai, *7th ASTM Symp. on Composite Materials, Testing and Design,* **ASTM STP 893,** J. M. Whitney, Ed. (Am. Socy. Testing and Maths., Philadelphia, 1986).
6. H. Chai, *Engineering Fracture Mechanics,* **20,** 413 (1986).
7. S. Mall and G. Ramamurthy, *Int. J. Adhesion and Adhesives,* **9,** 33 (1989).
8. S. A. Hamoush and S. H. Ahmad, *Int. J. Adhesion and Adhesives,* **35,** 171 (1989).
9. D. W. Schmueser and M. L. Johnson, *J. Adhesion,* **32,** 171 (1990).
10. G. Fernuld and J. K. Spelt, *Int. J. Adhesion and Adhesives,* **11,** 213 (1991).
11. G. Fernuld and J. K. Spelt, *ibid,* **11,** 221 (1991).
12. D. A. Schupp and W. W. Gerberich, *J. Adhesion,* **35,** 269 (1991).
13. H. R. Daghyani, L. Ye, Y.-W. Mai and J. S. Wu, *J. Mater. Sci. Lett.,* **13,** 1330 (1994).
14. R. F. Wegman, *Surface Preparation Techniques for Adhesive Bonding* (Noyes, Park Ridge, NJ, U.S.A., 1989), pp. 269–283.

15. J. R. Rice and G. F. Rosengren, *J. Mech. Phys. Solids*, 2 (1968).
16. Habbit, Karlsson and Sorensen, *ABAQUS User's Manual*, (Pawtucket, RI, USA. 1989).
17. W. D. Bascom and D. L. Hunston, *Treatise on Adhesion and Adhesives*, Robert. L. Patrick, Ed. (Marcel Dekker Inc., New York, U.S.A, 1989), pp. 123–185.
18. D. A. Bigwood and A. D. Crocombe, *Int. J. Adhesion and Adhesives*, **9**, 229 (1989).
19. J. N. Sultan, R. C. Laible and F. J. McGarry, *Appl. Polym. Sci.*, **6**, 627 (1971).
20. J. N. Sultan and F. J. McGarry, *Polym. Engng. & Sci.*, **13**, 29 (1973).
21. H. R. Daghyani, L. Ye and Y.-W. Mai, *J. Adhesion*, this issue.
22. S. S. Wang, J. F. Mandell and F. J. McGarry, *J. Fracture*, **14**, 39 (1978).
23. G. P. Anderson, S. J. Bennett and K. L. Devries, *Analysis and Testing of Adhesive Bonds* (Academic Press, New York, 1977).
24. J. H. Crews, Jr., K. N. Shivakumar and I. S. Raju, *Adhesively Bonded Joints: Testing and Design*, **ASTM STP 981**, W. S. Johnson, Ed. Am. Socy. Testing and Matls., (Philadelphia, 1988), pp. 119–132.
25. S. Yamini and R. J. Young, *J. Mater. Sci.*, **15**, 1823 (1980).
26. J. M. Scott and D. C. Phillips, *J. Mater. Sci.*, **10**, 551 (1975).
27. A. F. Yee and R. A. Pearson, *J. Mater. Sci.*, **21**, 2462 (1986).
28. S. Kunz-Douglass, P. W. R. Beaumont and M. F. Ashby, *J. Mater. Sci.*, **15**, 1109 (1980).